Case Studies in Thermal Engineering 59 (2024) 104479

Contents lists available at ScienceDirect

Case Studies in Thermal Engineering

journal homepage: www.elsevier.com/locate/csite

A case study on effect of twisting technique on heat transfer characteristics in a twisted oval helical tube

Mahdy Elsayed [a,b], Muhammad Sultan [c], Fahid Riaz [d], Manoj Kumar Agrawal [e], Mohammad Altaf [f], Nehad Ali Shah [g,***], B. Nageswara Rao [h,**], Li Zhang [i,*]

[a] Department of Environmental Engineering, School of Architecture and Civil Engineering, Chengdu University, Chengdu, 610106, China
[b] Department of Agricultural Engineering, Faculty of Agriculture, Cairo University, Giza, 12613, Egypt
[c] Department of Agricultural Engineering, Bahauddin Zakariya University, Multan, 60800, Pakistan
[d] College of Engineering, Abu Dhabi University, Abu Dhabi, United Arab Emirates
[e] GLA University, Mathura, UP, 281406, India
[f] Department of Chemistry, College of Science, King Saud University, P.O. Box 2455, 11451, Riyadh, Saudi Arabia
[g] Department of Mathematics, Saveetha School of Engineering, SIMATS, Chennai, 602105, Tamilnadu, India
[h] Department of Mechanical Engineering, Vignan's Foundation for Science, Technology &Research Deemed to be University, Vadlamudi, Guntur, Andhra Pradesh, 522213, India
[i] Sustainable Management of Natural Resources and Environment Research Group, Faculty of Environment and Labour Safety, Ton Duc Thang University, Ho Chi Minh City, Viet Nam

ARTICLE INFO

Handling Editor: Huihe Qiu

Keywords:
Twisting technique
Oval helical tube
Elliptical cross section
Heat exchanger
Entropy generation

ABSTRACT

Efficient transfer of energy is an important issue addressed by numerous scholars in the literature and various methods have been proposed for enhancing the heat transfer efficiency in heat exchangers. Among many different heat exchangers, helical tubes are one of the most prevalent types of heat exchangers which have many applications in industry. In a case study, effect of twisting technique on the heat transfer in a helical tube with oval cross section has been investigated numerically and the results have been compared with simple circular cross section helical tube. Effect of cross section aspect ratio and twisting ratio in different flow Reynolds numbers has been considered. Results have been presented in terms of Nusselt number, friction factor, PEC, entropy generation and contours of velocity, streamlines and temperature. Results indicate that twisting technique can significantly enhance the heat transfer and all cases have PEC values of above unit which indicates superiority of this method. Also the velocity contours and streamlines indicate that using twisting technique result in higher mixing in the flow which is the reason for higher heat transfer characteristics in twisted oval helical tubes.

1. Introduction

Energy crisis is the most important challenge that human kind is experiencing [1]. Depletion of fossil fuel resources and growth of population which has resulted excessive exploitation of natural resources, have urged scientists to discover methods for replacing the natural resources with the renewable energy resources for energy production [2–4] and suggest new methods for optimized consumption of energy [5–7]. Heat transfer enhancement of heat exchangers, due to its various engineering applications and the importance of

* Corresponding author.
** Corresponding author.
*** Corresponding author.
E-mail addresses: nehadali199@yahoo.com (N.A. Shah), director_ies@vignan.ac.in (B. Nageswara Rao), Lizhangna63@gmail.com (L. Zhang).

https://doi.org/10.1016/j.csite.2024.104479
Received 19 January 2024; Received in revised form 22 April 2024; Accepted 30 April 2024
Available online 1 May 2024

reducing energy consumption in various systems, has been one of the interesting topics for researchers in recent years [8][9,10]. Numerous methods have been suggested in the literature to enhance the overall performance of heat exchangers [11–13], the most important of which is to improve performance through optimal geometric design.

Due to various engineering applications, many studies have been conducted by researchers in order to achieve higher efficiency in helical heat exchangers. Energy storage potential of a helical heat exchanger installed on an air handling unit has been explored by Almitani et al. [14]. Cao et al. [15] numerically studied the overall performance of a double helical tube heat exchanger with circular depressions on the tubes. Exergy analysis of a helical coil heat exchanger coupled with a parabolic trough solar collector has been carried out by Chater et al. [16]. Li et al. [17] also conduted another exergy analysis on a corrugated spiral tube used in a solar pond. Based on thermal performance of Metal-hydride reactor, Eisapour et al. [18] provided an optimal design of a helical coil heat exchanger. Halawa and Tanious [19] utilized an elliptical tube in a helically coiled heat exchanger to improve thermal performance of it at turbulent flow regime. Among their under consideration parameters, they reported a significant augmentation of Nusselt number by decreasing the aspect ratio of elliptical tube. Hasan et al. [20] provided a numerical study around the impact of geometrical parameters of a helical heat exchanger containing nanofluids on the thermal performance enhancement. They considered different heating conditions to find the most efficient case, and according to their results, geometrical parameters play a key role on the thermal performance of heat exchanger. Lebbihiat et al. [21] analyzed thermal performance of a helical ground-air heat exchanger and provided both experimental and numerical results. The authors reported that the efficiency of heat exchanger is highly dependent on the thermal conditions. Heat transfer process of a helical heat exchanger was modeled by Missaoui et al. [22] in order to examine the effect of condenser coil design on overall performance of it. Cao et al. [23] investigated effect of corrugation in a helical tube in tube helical heat exchanger and reported a considerable increase in the heat transfer by using corrugation technique. Yanlin et al. [24] in a most recent investigation addressed effect of different cross section modifications on the fluid flow and energy transfer of a helical tube and reported significant enhancement of heat transfer by using this method. Also several other studies have been conducted recently addressing effect of geometrical modifications including corrugations and twisted tapes on the heat transfer enhancement in heat exchangers [25,26].

Some researchers have utilized twisted tubes and twisted tapes in order to increase the heat transfer rate of heat exchangers. Lu and Song [27] explored the influence of aspect ratio and twist ratio on the thermal performance of a twisted annulus placed between two twisted elliptical tubes. They reported effective secondary flow formation and an increase in Nusselt number of 157%. Luo et al. [28] numerically investigated the heat and fluid flow of a co-twisted double-pipe heat exchanger in laminar flow regime with different twist pitches. The authors considered the effect of the twist pitch ratio on the thermal performance of the heat exchanger and reported that increasing the twist pitch ratio increases the heat rate at first, and then decreases with further increasing. Yu et al. [29] conducted a numerical study to analyze the thermal-hydraulic performance of a twisted elliptical pipe with various wire coils at turbulent flow. According to their results, the authors concluded that the direction of the coil has a significant effect on the overall performance of the twisted pipe. Zhu et al. [30] studied the impact of using a twisted tape within a thermoelectric generator heat exchanger by means of finite-element method. They investigated the geometrical parameters affecting the overall performance including the length, twist ratio, and radius of the twisted tape. According to their results, their proposed heat exchanger increases the net power by 10.41% and the efficiency by 22.51%. Ali and Jalal [31] evaluated the heat transfer and fluid flow of a double-pipe heat exchanger with a twisted inner pipe for both parallel and counter flows. The parameters investigated by the authors include the number of twists and Reynolds number. Examining their results indicates that the use of twisted pipe improves the overall performance of the heat exchanger, and the highest value of Nusselt number is obtained in the case with the highest number of twists. Fallah Najafabadi et al. [32] analyzed a twisted double pipe heat exchanger including phase change material as a solar energy storage unit. The parameters that the authors investigated are pipe position, twisting, and cross-sectional geometry. According to their calculated results, the heat transfer rate is notably dependent on the geometry of the cross-section and the best thermal performance is obtained using the 3-lobed cross-sectional geometry. Kim et al. [33] worked on heat transfer in an oval twisted tube in both laminar and turbulent flow regimes and studied effect of different Reynolds numbers and different twisting ratios and reported that although using twisting technique may increase the friction factor, but it has a considerable influence on the heat transfer too. Chang et al. [34] utilized twisting technique in a helical tube by using a square cross section with different amounts of twisting pitches and reported that higher twist ratios can result in better heat transfer in helical tubes with square cross sections. Wu et al. [35] conducted a numerical study to verify effect of twisting technique in an elliptical tube and reported how twisting oval cross section may affect heat transfer and fluid flow in a straight tube. In a most recent study, Eiamsa et al. [36] studied an oval ribbed tube with different pitches and twisting ratios. They reported that combination of swirling flow generation and flow separation and reattachment behind the ribs would result in higher mixing of the flow and better heat transfer performance.

According to previously mentioned studies most of which are of the most recent works reported in the literature, it could be perceived that helical tubes have numerous application in industrial applications for heat transfer purposes and a great effort has been dedicated so far to introduce novel techniques to enhance the efficiency of heat transfer in helical tubes. On the other hand, using twisting method in oval cross sections of tubes with different aspect ratios is another method to enhance flow mixing and increase the heat transfer efficiency. However, according to the aforementioned literature review and to the authors' best knowledge, the twisting technique has never been applied to helical tubes with oval cross section and its aspects remain mostly obscure. In this regard, present study is aimed at analyzing heat and fluid flow characteristic in a helical heat exchanger with elliptical twisted tubes. The influence of oval cross section aspect ratio and twisting ratio of helical tube in different Reynolds numbers have been verified in this work and results including flow and heat transfer parameters have been reported.

2. Problem statement and methods

2.1. Model definition and boundary conditions

The base model considered in this work is a helical tube with circular cross section in which the diameter of the tube has been taken to be 10 mm and the helical pitch and the diameter of the helix have been taken to be 20 mm and 100 mm respectively. In order to study effect of the cross section aspect ratio and twisting technique on the heat transfer to the fluid, 4 different aspect ratios each of which with 4 different twisting pitches have been investigated alongside the base case which in overall, total of 17 distinct cases have been studied. The flow rates were ranging between 2 and 10 L/min which are associated with the Reynolds of 5600–28000. The different aspect ratios are 1.5, 2, 2.5, 3 and 3.5 and the different angles used for the twisting are 360 °, 720 °,1080 ° and 1440 °. The twisting angle is defined as the angle of twist between the inlet of the tube and the outlet of the helical tube as if for a twist angle of 720 °, the whole body of the tube between the inlet and outlet has been twisted two times. Fig. 1 depicts the geometrical model and the related geometrical parameters and dimensions. Fig. 1A presents view of the model with different twist angles while the dimensions of the base helix are indicated on the base model. Fig. 1B demonstrates the different aspect ratios studied with the parameters related to the major and minor axis of the elliptical cross sections. It is to be noted that the aspect ratio has been calculated as follows:

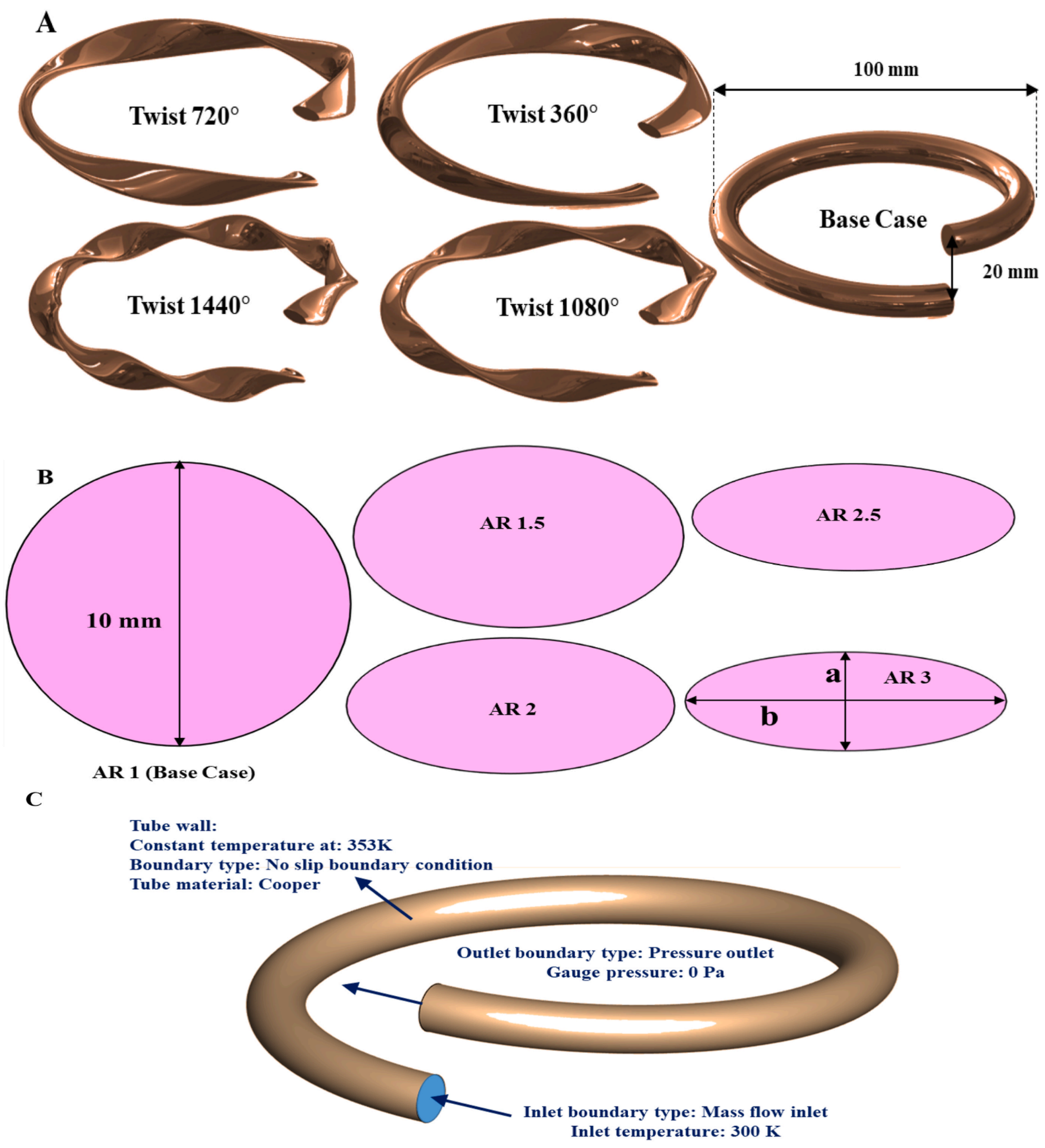

Fig. 1. Presentation of the studied model with different aspect ratios and twisting angles. A: The different twisting angles applied on the case with AR = 3 along with the dimensions of the helically coiled heat exchanger including the pitch and diameter of the helix. B: Different aspect ratios used for the model with the related parameters. C: Graphical presentation of the boundary conditions including the inlet, wall and outlet.

$$AR = b/a \tag{Eq.1}$$

In which the parameters “a” and “b” have been demonstrated in Fig. 1B. The dimensions of the major and minor diameters along with the cross section area of the ellipse have been presented in Table 1. As the hydraulic diameter of the main circular tube as the base case has been considered to be 10 mm, the minor and major diameters of the elliptical models have been selected in such a way that the hydraulic diameter in all cases remains the same. The hydraulic diameter of ellipse is calculated as follows:

$$D_h = \frac{\sqrt{2}\, ab}{\sqrt{a^2 + b^2}} \tag{Eq.2}$$

In the above equation, D_h is the hydraulic diameter and the parameters “a” and “b” denote the major and minor diameters of the ellipse as shown in Fig. 1B. The dimensionless parameter Reynolds number is an indication of the flow regime in the tube which is calculated based on the following equation:

$$Re = \frac{\rho V D_h}{\mu} = \frac{4\dot{m}}{\pi D_h \mu} \tag{Eq.3}$$

According to Eq.3, the Reynolds number in a tube is dependent to the flow rate and the hydraulic diameter of the tube. Keeping the hydraulic diameter constant in all cases makes it feasible to make comparisons between different cases with similar flow rates due to equal amount of Reynolds.

The inlet flow was defined with the “mass flow inlet” boundary condition with the flow rates ranging between 2 and 10 L/min with a constant temperature of 300K and the outlet of the tube was denoted with the “pressure outlet” boundary condition with zero-gauge pressure at the outlet which means the flow is in contact with the atmosphere at the outlet. While flowing inside the tube, the heat transfer fluid receives energy from the tube wall with constant temperature of 353K. The boundary conditions have been graphically presented in Fig. 1C.

2.2. Numerical method

In order to solve the governing equations of turbulent flow with heat transfer, the commercial CFD code ANSYS Fluent has been adopted and the results of the fluid flow characteristics were analyzed in the post-processing software CFD-Post and Tecplot. The governing equations in tensor form for a turbulent flow with the steady state conditions are as follows:

Continuity equation:

$$\frac{\partial}{\partial x_i}\left(u_i\right) = 0 \tag{Eq.3}$$

In which u_i represents the velocity vector in tensor form.

Momentum equation:

$$\frac{\partial}{\partial x_j}\left(\rho u_i u_j\right) = -\frac{\partial P}{\partial x_i} + \frac{\partial}{\partial x_j}\left[\mu\left(\frac{\partial u_i}{\partial x_j} + \frac{\partial u_j}{\partial x_i}\right)\right] + \frac{\partial}{\partial x_j}\left(-\rho\overline{\acute{u}_i \acute{u}_j}\right) \tag{Eq.4}$$

Where in the above equation, μ, ρ and $\acute{u}$ are the dynamic viscosity and density of the fluid and the fluctuant terms of the velocity vector in tensor form.

Energy equation:

$$\frac{\partial}{\partial x_i}\left(\rho u_i T\right) = \frac{\partial}{\partial x_j}\left[\left(\frac{\mu}{Pr} + \frac{\mu_t}{Pr_t}\right)\frac{\partial T}{\partial x_j}\right] \tag{Eq.5}$$

Where Pr and Pr_t are the fluid Prandtl number and the turbulent flow Prandtly number and μ_t is the turbulent flow viscosity. T in Eq.3 represents temperature.

Eq. (2) is the Reynolds-Averaged Navier-Stokes (RANS) equation which has been derived by considering the fluctuant terms of the turbulent flow in velocity vector resulting in addition of an extra term to the right side of the equation which is called the Reynolds

Table 1
Geometrical dimensions of different cases.

AR	a (mm)	b (mm)	Area (mm2)
1	10	10	78.53
1.5	8.5	12.74	21.3
2	7.9	15.8	24.51
2.5	7.6	19	28.36
3	7.44	22.32	32.61

stress term ($\rho\overline{\acute{u}_i\acute{u}_j}$). In order to close the set of equations to fin the flow field variables, the Reynolds stress term should be properly modeled. To model this term, the Boussinesq hypothesis has been employed in this work which considers a relation between the Reynolds stress and the mean velocity gradients:

$$\left(-\rho\overline{\acute{u}_i\acute{u}_j}\right) = \mu_t\left(\frac{\partial u_i}{\partial x_j} + \frac{\partial u_j}{\partial x_i}\right) \tag{Eq.6}$$

The turbulent viscosity in Eq. (4) (μ_t) is calculated by the following equation:

$$\mu_t = \rho C_\mu \frac{k}{\varepsilon} \tag{Eq.7}$$

In Eq. (5), C_μ is a constant which is equal to 0.09 in this simulation. The terms k and ε are the turbulence kinetic energy and its rate of dissipation which should be calculated to close the system of governing equations. In order to obtain the k and ε terms, the standard k-ε turbulent model has been employed. According to this model, the terms k and ε are obtained by solving the following equations:

The k-equation:

$$\frac{\partial}{\partial x_i}(\rho k u_i) = \frac{\partial}{\partial x_j}\left[\left(\mu + \frac{\mu_t}{\sigma_k}\right)\frac{\partial k}{\partial x_j}\right] + G_k - \rho\varepsilon \tag{Eq.8}$$

The ε-equation:

$$\frac{\partial}{\partial x_i}(\rho \varepsilon u_i) = \frac{\partial}{\partial x_j}\left[\left(\mu + \frac{\mu_t}{\sigma_\varepsilon}\right)\frac{\partial \varepsilon}{\partial x_j}\right] + C_{1\varepsilon}\frac{\varepsilon}{K}G_k + C_{2\varepsilon}\rho\frac{\varepsilon^2}{k} \tag{Eq.9}$$

G_k is the turbulent kinetic energy generation rate. In the above equations, the terms σ_k and σ_ε are the turbulent Prandtl numbers for k and ε respectively and are constant values. In the standard k-ε model, the values of constants of σ_k, σ_ε, $C_{1\varepsilon}$ and $C_{2\varepsilon}$ are 1, 1.3, 1.44 and 1.92 respectively.

One of the most important regions which may significantly affect the modeling results is the near wall region where the turbulence fluctuations are significantly affected by the presence of the walls. On the other hand, the near wall region is assigned with large gradients of the flow parameters. Hence, in order to accurately predict the near wall parameters, EWT (Enhanced Wall Treatment) has been used as the near wall treatment method which requires a fine mesh at the boundaries of the tube with its y^+ being in the order of 5. Hence, very fine mesh has been generated on the walls of tube with a growing ratio toward the center of the tube as presented in Fig. 2B.

It should be noted that the SIMPLE scheme was utilized to couple the velocity and pressure and the PRESTO scheme was used for pressure interpolation. The second order upwind method was used for discretizing the momentum and energy equations. In order to have more accurate results, the convergence criteria for continuity, momentum and energy equations were set to 10^{-4}, 10^{-6} and 10^{-6}.

2.3. Mesh independence

Number of the mesh generated in the domain can significantly influence the accuracy and solution time. Hence, before running the final simulations, a mesh independence analysis should be performed. Different number of meshes were generated on the domain and the friction factor and Nusselt number which both are dimensionless numbers were evaluated by these meshes. Fig. 2 indicates variation of *Nu* and friction factor with increasing the number of computational grids. It could apparently be seen that the first three domains with 25k, 152k and 218k meshes generate a great variation in the results. However, when increasing number of grids from 218k to 408k, both the *Nu* and friction factor remain almost constant and further increment of the mesh number causes no change on the results. Hence, in all further simulations, the number of cells have been set on 408000 to have the highest accuracy with lowest computational cost. It is noteworthy to mention that in this work, a fully structured hexahedral mesh has been generated with highest quality possible.

It should be noted that the mesh independence analysis has been evaluated with the most critical case which is the case with highest aspect ratio (AR = 3) and highest twist angle (1440 °) to avoid loss of accuracy for more complicated models. A view of the generated mesh on the model with AR of 3 and twist angle of 1440 has been demonstrated in Fig. 3B.

3. Results

3.1. Validation

As numerical errors are inevitable in numerical simulations, it is critical to make a comparison between the numerical results and the experimental results present in the literature. Hence, in this study, the results obtained by numerical simulations have been compared against most credible experimental works in the literature. The friction factor as a dimensionless parameter obtained by the simulations and the works of Ito [37], Mishra and Gupta [38] and Mori and Nakayama [39] have been compared. Another dimensionless parameter reported in this work which represents the convective heat transfer is Nusselt number which has been compared against the works of Hardik et al. [40] and Schmidt and Eckehard [41].

A)

B)

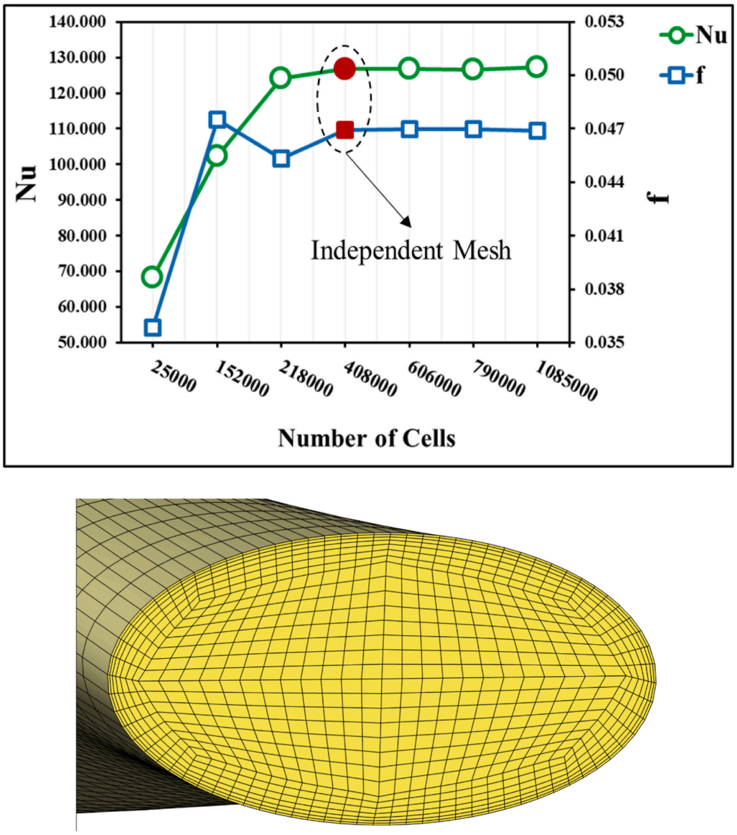

Fig. 2. A) Mesh independence analysis results for Nusselt number and friction factor for different cell numbers, **B)** A view of the structured mesh generated on the model.

Fig. 3A presents the comparison of friction factor with the works of Ito [37], Mori and Nakayama [39] and Mishra and Gupta [38]. It is clearly observed that the results have very good agreement with the experimental works and the deviation of the numerical results can be assumed negligible. The deviation increases with increasing the flow rate and the maximum deviation is observed at the highest flow rate of 6L/min which is with the work of Mishra and Gupta [38] and is 7.52% which is totally acceptable for numerical simulations. While the error with other works is far below this quantity which shows the reliability of the obtained results. It should also be noted that each of the experimental works have also some errors which is originated from different sources such as the accuracy of the devices, the conditions of experiments and etc. Hence, the minor differences in the experimental works themselves is plausible. At the same time, it is observed that the present results totally fall within the experimental results range and it is another reason to deduce the credibility of the numerical method.

The friction factor represents the hydraulic characteristics of the flow and compatibility of this parameter with the experimental works denotes validity of the solution of the flow field by numerical method adopted in this work. Although, in order to assess the validity of the solution of the heat transfer by the fluid flow, the Nusselt number has also been compared against the experimental works. Fig. 3B presents the comparison of the Nusselt number calculated by the numerical solution with the works of Hardik et al. [40] and Schmidt and Eckehard [41]. It is observed that the results are in the same range as the experimental works and the deviation is below 10% at all points except the flow rate of 6L/min. At this flow rate, a deviation of 13.43% is observed with the work of Hardik et al. [40] while the deviation of Nusselt number with the work of Schmidt and Eckehard [41] at all flow rates is below 7%.

The numerical errors with each of the experimental works mentioned in this section whether for the friction factor or the Nusselt number have been presented in Table .2. It is to be noted that the errors presented in this table have been calculated based on Eq. (10). According to Fig. 3 and Table 2 and it could be concluded that the present numerical method adopted for the simulations is totally reliable and the results have good compatibility with the experimental works. Hence, the method has been used for the rest of simulations.

$$Err = \frac{f_{Numerical} - f_{Experimental}}{f_{Experimental}} * 100 \tag{Eq.10}$$

A)

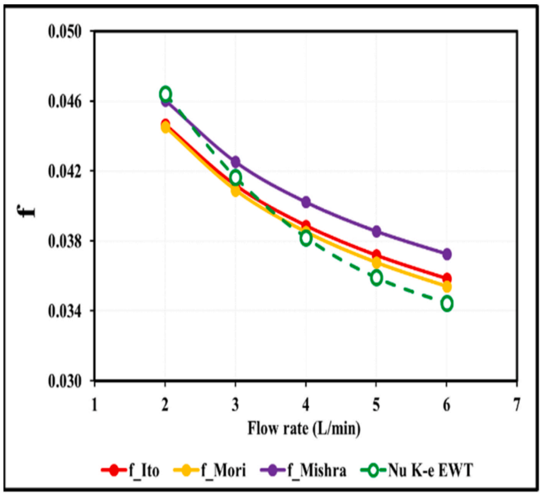

B)

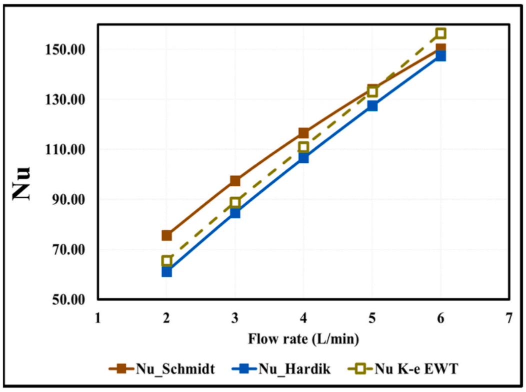

Fig. 3. The validation results compared with experimental works in the literature. **A)** Comparison of the friction factor with works of Ito, Mori and Nakayama, and Mishra and Gupta. **B)** Comparison of Nusselt number with the works of Schmidt and Eckehard and Hardik et al.

Table 2
Friction factor and Nusselt discrepancy with experimental works.

Flow rate (Kg/min)	Reynolds	Friction Factor Errors			Nusselt Errors	
		Ito [37]	Mishra and Gupta [38]	Mori and Nakayama [39]	Hardik et al. [40]	Schmidt and Eckehard [41]
2	5600	3.91	0.77	4.23	6.93	13.43
3	11200	1.10	2.08	1.79	4.94	8.80
4	16800	1.74	5.04	0.82	4.01	4.95
5	22400	3.41	6.86	2.32	4.45	0.75
6	28000	3.87	7.52	2.65	6.04	4.01

3.2. Results

In this section, the results of the flow parameters regarding the first and second laws of thermodynamics are presented and discussed. Fig. 4 represents the friction factor variation in different cases with different aspect ratios and different twist angles at different Reynolds numbers ranging between 5600 and 28000. The friction factor is calculated as:

$$f = \frac{2 * \Delta P * D_h}{\rho * L * V^2} \tag{Eq. 11}$$

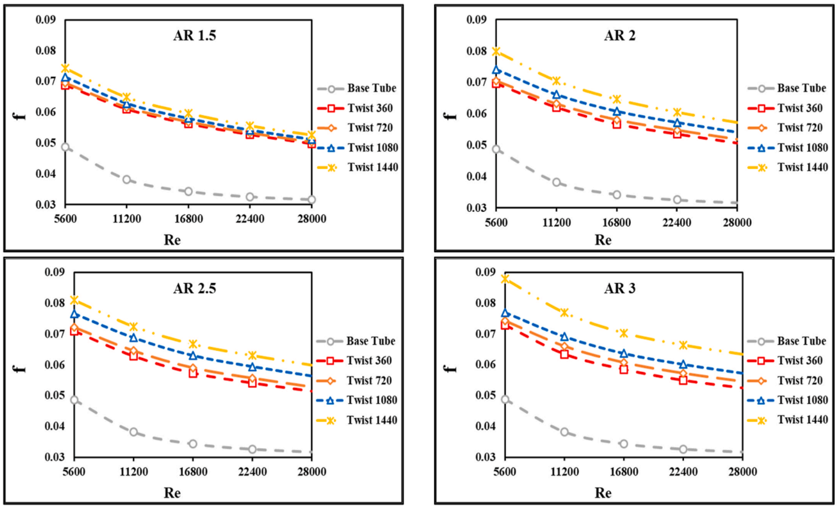

Fig. 4. Friction factor variation with Reynolds number for different aspect ratios (AR) and twist angles for different amounts of Reynolds.

In which "f" is the friction factor, ΔP is the pressure loss from the inlet to the outlet of the tube, D_h is the hydraulic diameter of the tube, L is the length of the tube, ρ is the density of the operating fluid and V is the mean velocity of the fluid at the inlet.

According to Fig. 4, it is observed that the friction factor in all cases with different pitches and aspect ratios reduces as the flow Reynolds number increases. It is an obvious observation because according to the friction factor equation (Eq. 11), increasing the Reynolds number although increases the pressure loss, but at the same time the velocity of the fluid increases too, which means the denominator of the equation grows at a greater pace than the numerator and results in reduction of the friction factor. However, one main finding according to Fig. 4 is that in all aspect ratios, the friction factor is directly related with twist angle of the tube as it could be seen by comparing the friction factor in different twist angles that the friction factor increases as the tubes get twisted with higher angles which means the tubes with twist angle of 1440 have the highest rate of friction factor among all cases with different aspect ratios. It could be realized that higher twist of the tubes is accompanied with more difficult flow of fluid inside the tubes and the shear stress enhancement which results in higher pressure drop and higher friction factor. It is to be noted that twisting the tube also increases the tube surface which is in contact with the fluid and results in higher amount of friction between the fluid flow and the tube. Another point to extract from the results presented in Fig. 4 is the effect of aspect ratio on the friction factor. It is obvious that higher aspect ratios are associated with greater resistance against the flow of fluid inside the tube. As a result, it is observed that the magnitude of friction factor raises for same amounts of twist angles at higher aspect ratios, although this occurrence is more prominently observed for the higher twist angles. This is also figured out that the friction factor curves of different twist angles get separated and diverge from one another as the aspect ratio raises. It is seen that the curves are mostly close to each other in cases with aspect ratio of 1.5 but they are distanced from each other in the cases with aspect ratio of 3. This means increasing the aspect ratio not only increases the friction factor, but also results in its progressive growth at higher twist angles. Hence, it could be observed that the highest amount of friction factor is achieved for the case with aspect ratio of 3 at the twist angle of 1440.

Fig. 5 represents the variation of the ratio of Nusselt number in oval tubes to the Nusselt in the base tube (Nu/Nu_0) for different twist angles and different aspect ratios. According to Fig. 5, in all cases with all amounts of aspect ratios, the Nu/Nu_0 is higher than unit which means all of the cases have experienced a considerable augmentation of heat transfer and using the elliptical cross section technique has positive effect on the heat transfer in helical tubes. However, different cases associated with different amounts of twist angles and aspect ratios represent different heat transfer enhancement characteristics. When evaluating the heat transfer characteristics in terms of the twist angle, it is observed that the increasing the twist angle increases the Nu/Nu_0 ratio. As indicated in Fig. 5, the magnitude of the Nu/Nu_0 curves is higher for higher twist angles at each of the constant aspect ratios and this pattern is repeated almost in all of the curves for all amounts of aspect ratios. Also, it is observed that increasing Reynolds number from 5600 to 11200 enhances level of heat transfer ratio almost in all cases but further increment of Reynolds number results in an adverse effect on the Nu/Nu_0 and an extremum is observed in the Reynolds of 11200 after which the ratio of Nusselt number decreases to a certain value at the Reynolds of 22400 which a minimum is formed. By further increment of Reynolds number, the amount of Nu/Nu_0 increases at lower amounts of aspect ratio although the slope of increment in higher aspect ratios remains lower and at the aspect ratio of 3 which is the highest aspect ratio in this study, the Nu/Nu_0 remains constant after Reynolds of 22400.

Another feature revealed by Fig. 5 is that increasing aspect ratio is not beneficial for heat transfer enhancement since it is observed that the level of Nu/Nu_0 curves falls down by raising the aspect ratio. According to Fig. 5 (AR 1.5) the total amounts of Nu/Nu_0 at all twist angles are bounded between the amounts of 3.15–3.48 however by increasing the aspect ratio the whole curves shift downward to the point that in Fig. 5 (AR 3) the curves of different twist angles are bounded to the amounts of 2.18–2.58.

Figs. 4 and 5 were dealing with the pressure drop and heat transfer in the studied cases which are two of the most important flow characteristics in tubes. It is to be noted that the first one is an undesirable parameter which poses extra cost to overcome the loss of pressure while the second parameter which relates to heat transfer is a parameter that is tried to be improved as much as possible and

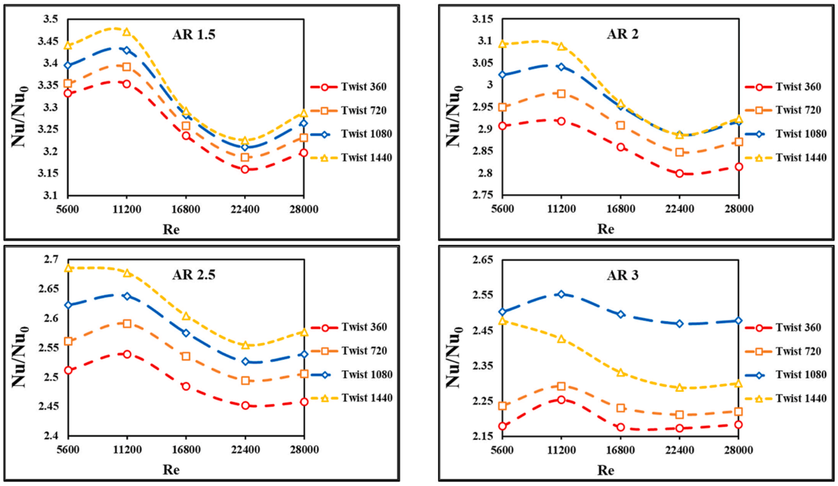

Fig. 5. Variation of the ratio of Nusselt to the Nusselt in the base case (Nu/Nu_0) with Reynolds number for different cases with different twist angles and aspect ratios.

is desirable to enhance in tubes. It is important to note that any method of heat transfer enhancement not only may augment the heat transfer rate as an advantage, but it may increase the pressure loss in the tube which is an undesirable phenomenon and causes extra expenses. Hence, the enhancement methods should be evaluated simultaneously in terms of both heat transfer and pressure drop to reveal if it is beneficial to use the method or not. To do so, the Performance Evaluation Criteria (PEC) is a good parameter which takes into consideration both the pressure drop and the heat transfer enhancement at the same time and is calculated as follows:

$$PEC = \frac{\frac{Nu}{Nu_0}}{\left(\frac{f}{f_0}\right)^{\frac{1}{3}}} \tag{Eq.12}$$

In the above equation, Nu and Nu_0 are the Nusselt number for the enhanced tube and the base tube and f and f_0 are the friction factor for the enhanced tube and the base tube. The PEC values above unit are regarded to be economically beneficial as they have a greater rate of heat transfer enhancement as a desired value in comparison with the loss of the pressure as an undesirable value which means the enhancement method has higher benefit than its loss. According to Fig. 6, it could be realized that all of the cases with all ranges of twist angles and Reynolds produce enhancement in heat transfer with the amount of PEC above unit which means the twisting technique for oval cross sections in helical tubes remains a positive effect on the heat transfer enhancement. However, the PEC values for each amount of aspect ratio reduces with increasing the twist angle which could be due to the higher amount of pressure drop at higher twist angles which is greater than the rate of heat transfer enhancement. In Fig. 5 it was revealed that the higher twist angles are associated with higher heat transfer enhancement despite the PEC results that higher twist angles indicate lower effectiveness for the enhancement method employed. It could be concluded that in applications where the heat transfer is the highest priority, increas-

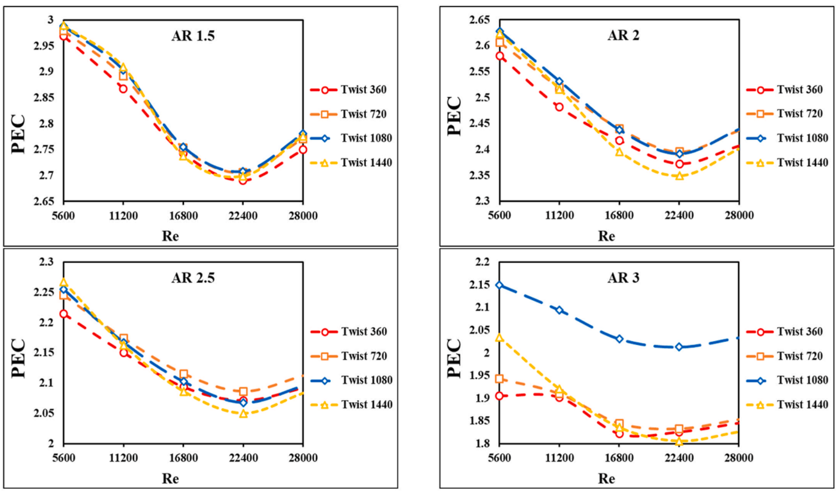

Fig. 6. Variation of the Performance Evaluation Criteria (PEC) with Reynolds number for different cases with twist angles at different aspect ratios.

ing the twist angle is recommended to achieve better heat transfer however for applications where the expenses is also important, it is better to employ tubes with lower twisting angles. It is also observed in Fig. 6 that increasing Reynolds number has negative effect on the PEC values and it could be figured out that lower Reynolds values return the best results when using the twisting technique for oval cross sections. Another point to note in Fig. 6 is that the level of curves drops for higher aspect ratios which is due to the lower amounts of Nusselt for higher aspect ratios as demonstrated in Fig. 5.

Fig. 7 represents the ratio of entropy generation in each case to the entropy generation in the base tube. Entropy generation is important as it indicates not only the heat transfer enhancement based on the first law of thermodynamics, but also it considers the second law as well. According to Fig. 7, lower aspect ratios are associated with lower amount of entropy generation, however as the aspect ratio raises, the amount of entropy generation ratio also increases and it is observed that the highest entropy generation ratio reaches amount of 1.75 for AR = 3. Also it is observed that increasing the twist angle remains an undesirable effect on the entropy generation and as indicated in Fig. 7, in all amounts of aspect ratios, the entropy generation ratio increases with increasing the twist angle. Also the Reynolds number increment results in raise in the entropy generation however further increment of Reynolds number causes the fluctuation in the amount of entropy generation and again raises the entropy generation at higher Reynolds number. According to Figs. 6 and 7, it could be concluded that the most efficient point for using the twist technique for heat transfer enhancement is at lower Reynolds as the PEC is maximum and the entropy generation ratio is minimum in this region which satisfies both the first law and second law of thermodynamics.

Fig. 8 demonstrates the velocity contours in different cases with different twist amounts at the 14 consecutive cross sections prior to the outlet section. These cross sections can help better realize and analyze the dynamics of flow and effect of twisting the cross sections on the flow field. It is observed that in the base tube, the effect of centrifugal force is evident as it is seen that the flow velocity is higher at the outer bend in comparison with the inner bend. Also a thin layer is observed with lower velocity at the vicinity of the wall which is due to the boundary layer development. In the base tube where only the centrifugal force is dominant, the velocity distribution is not uniform and the outer bend velocity is rather higher than the inner bend. However, in the twisted cases the high velocity region occurs at the corner in some of the depicted cross sections. It demonstrates that the local twist is also effective in generating a local centrifugal force in spite of the bend centrifugal force. An important point to note according to Fig. 8 is that increasing the amount of twist results in disappearance of a high velocity hotspot and the high velocity region encompasses a higher area at each cross section, as if the velocity is more uniformly distributed over each cross section. Comparing the case with twist 360 and the one with twist of 1440 in Fig. 8 reveals that the high velocity region in the vicinity of the pole of the tube has pervaded in other sides in case with twist 1440 and a bigger area is flowing with higher velocity. This phenomenon can also be observed in Fig. 9 in which the flow streamlines in consecutive cross sections prior to the outlet of the tube have been depicted for different cases with different amount of twist. It is clearly seen that the twist of tube has totally altered the streamline patterns in the base tube. In the base tube, the counter rotating vortices at each cross section is evident which is famous as dean vortices. But in the cases with twist of the tubes, the previous prevalent pattern of the counter rotating vortices has vanished and only in some cross sections one vortices is formed and in most of other cross sections none of the vortices is generated. This indicates effect of local centrifugal force due to twist of the tube cross section which eliminates the ordinary Dean vortices and creates new patterns.

Fig. 10 represents the temperature contours in consecutive cross sections prior to the outlet of the tube in different cases with different amounts of twist. According to the presence of centrifugal force, it is evident that in the base tube the fluid at the outer bend has lower temperature due to the higher velocity in that region. Because the flows with higher velocity have less time to exchange energy with the high temperature walls which consequently gain lower amounts of thermal energy, while in the inner bend the fluid flows slowly in comparison with the outer bend and gains higher amount of energy which is the reason for higher temperature at the

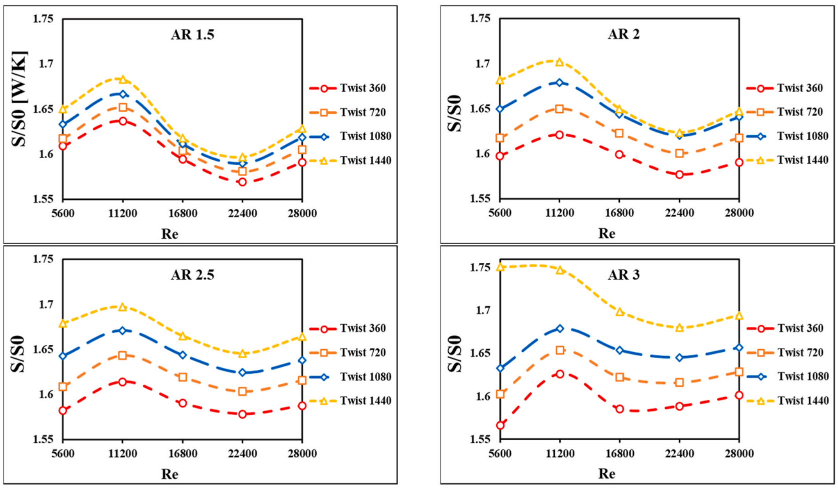

Fig. 7. Variation of the entropy generation ratio (the enhanced tube entropy generation to the base tube entropy generation) with Reynolds number in different cases with different aspect ratios and twist angles.

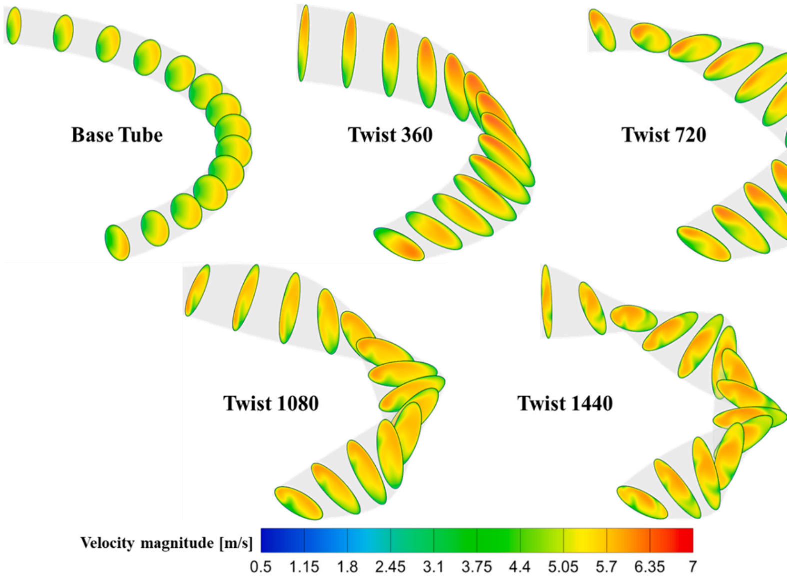

Fig. 8. Velocity contours for different cases for Re = 28000 at consecutive cross sections at the outlet section of the tube.

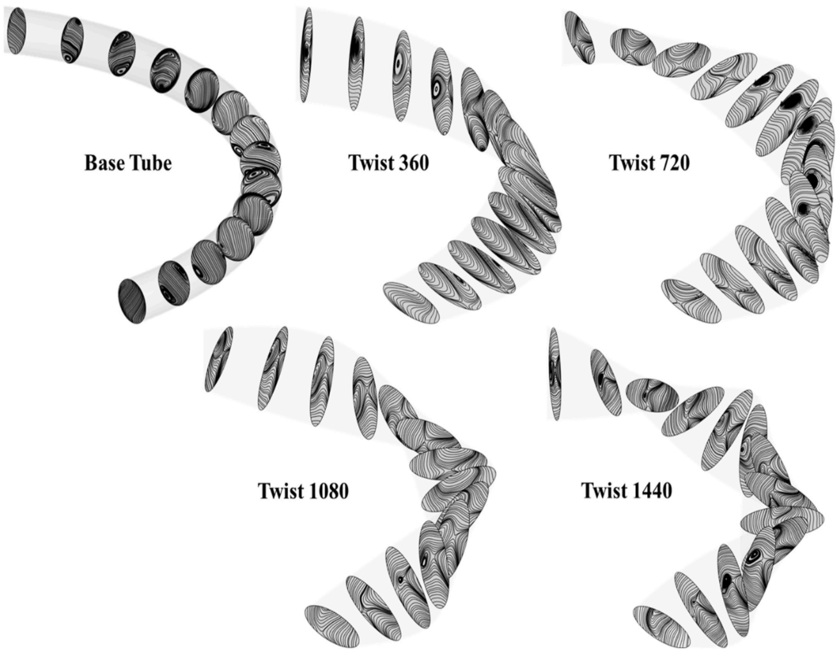

Fig. 9. Flow streamlines on consecutive planes at the outlet section of the tube at different cases.

inner bend. However, when the oval cross section gets twisted along the axis of the tube, the flow gets much better mixed and the fluid in the vicinity of the wall are more efficiently replaced and the flow has better potential to gain the energy from high temperature walls which not only increases the heat transfer rate, but also makes the energy distribution more evenly among the fluid flow. This could be easily seen in Fig. 10 which the whole cross sections in the twisted tubes have approximately equal temperature. It is also important to note that presence of high velocity fluid over the cross section of the twisted tubes (Fig. 8) is a good sign for local mixing of the fluid and higher efficiency for heat transfer. This finding is in good agreement with the Nusselt number reported in Fig. 5 where the twisted cases had shown higher performance in comparison with the base tube.

Fig. 11 depicts the flow streamlines colored by velocity magnitude for different cases including the base case and the twisted cases with different amounts of twist. The streamlines in the base tube clearly show the formation of secondary flow which is due to the curvature of the tube and the centrifugal force exerted on the fluid. As the fluid reaches the outer bend, presence of curve makes the fluid to generate vortices and move toward the inner bend which results in generation of counter rotating vortices which are so called the Dean vortices. This phenomenon is previously observed in the flow streamlines depicted on the cross sections in Fig. 9.

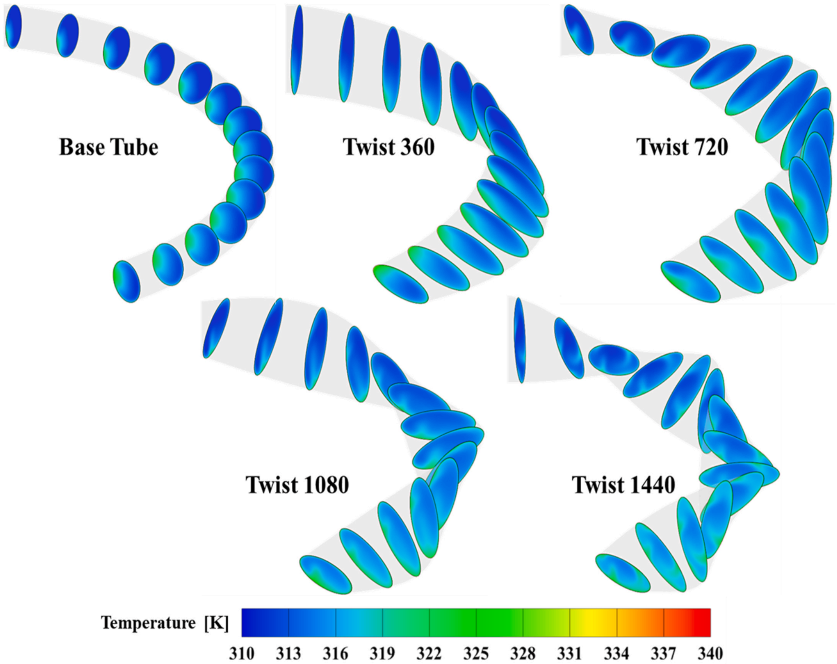

Fig. 10. Temperature contours for different cases for Re = 28000 at consecutive cross sections at the outlet section of the tube.

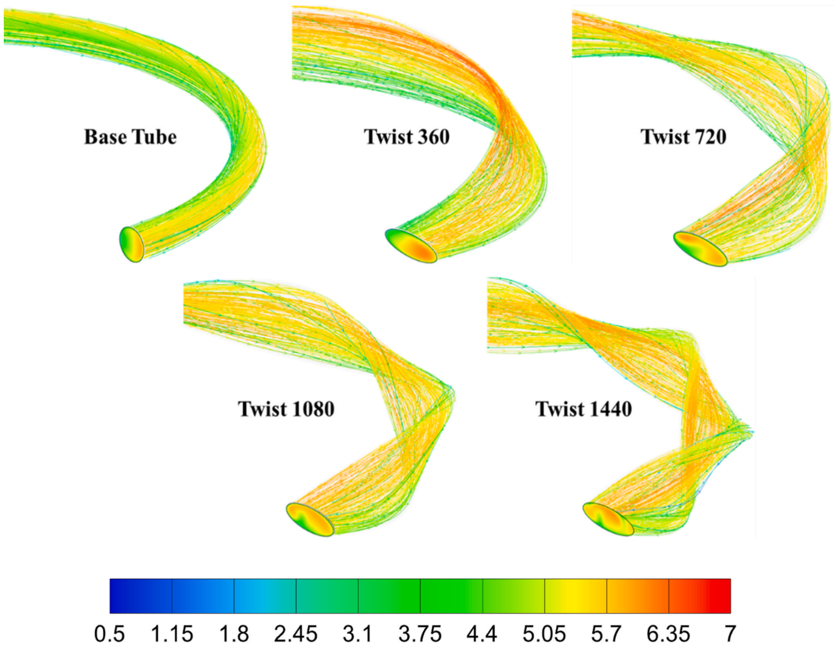

Fig. 11. Flow streamlines for different cases for Re = 28000.

The important point to note is the effect of twisting on the streamlines. It can be observed in the tube with twist of 360 in Fig. 11 that the streamline patterns have modified in comparison with the base tube. The secondary flow has been affected by the twist in cross section and the previous ordinary counter rotating vortices have disappeared, instead the streamlines have been mostly adjusted with the twisting of the tube. As the 360 ° twist doesn't make such great inclination in tube bend, the streamlines are more parallel however increasing the twist will make intense influence on the streamlines in such a way that in the case with twist of 1440 a very complicated and distorted formation of streamlines are observed. Also as mentioned in Fig. 8, presence of swirls causes the momentum to get better distributed along each cross section which this phenomenon is also observed in Fig. 11.

4. Conclusion

In this work, effect of twisting oval cross section in a helical tube on the flow field and heat transfer characteristics has been studied numerically. Different cross sections with 4 different aspect ratios and different amounts of twisting have been assessed to find out how increasing the aspect ratio or increasing the twisting of the cross section may influence the fluid flow and more importantly the heat transfer characteristics. The governing equations were solved using the commercial CFD code, ANSYS Fluent and the results have been presented in terms of friction factor, Nusselt number, entropy generation and PEC and the flow streamlines, temperature and velocity contours have also been depicted to help for better analysis of the problem. The key findings in this work are as follows.

- Using twisting technique along with oval cross sections showed good impact on the heat transfer and cases with twisted cross section had better heat transfer characteristics. While along with heat transfer enhancement, the pressure drop also increases accordingly.
- The Nu/Nu_0 ration in twisted cases was above unit and in some cases showed amount of 3.48 which shows twisting can perfectly enhance heat transfer up to 3.48 times the Nu in base tube.
- The PEC for all cases is above unit which shows economic benefit of using twisting technique for enhancing twisting technique in helical tubes with oval cross sections. The highest PEC achieved is 3 which relates to the case with aspect ratio of 1.5 with twist of 1440 °.
- It is revealed that increasing aspect ratio has adverse effect on the heat transfer due to higher amount of pressure loss and increasing the amount at the denominator of the PEC equation while increasing twist has optimal effect and cases with higher twist show higher rate of PEC and heat transfer.
- The cases with cross section twist help better mixing of the flow and hence have better heat transfer characteristics which has been indicated in the velocity contours.
- According to the temperature contours, the energy can better disperse along the whole cross section of the tube which shows better mixing of the fluid and better heat transfer characteristics.

CRediT authorship contribution statement

Mahdy Elsayed: Conceptualization, Writing – original draft, Writing – review & editing. **Muhammad Sultan:** Data curation, Writing – original draft. **Fahid Riaz:** Formal analysis, Writing – review & editing. **Manoj Kumar Agrawal:** Investigation, Methodology. **Mohammad Altaf:** Validation, Writing – original draft. **Nehad Ali Shah:** Project administration, Resources. **B. Nageswara Rao:** Writing – review & editing. **Li Zhang:** Writing – original draft, Validation, Supervision.

Declaration of competing interest

The authors declare that they have no known competing financial interests or personal relationships that could have appeared to influence the work reported in this paper.

Data availability

Data will be made available on request.

Acknowledgments

- The current work was supported by Chengdu University's start-up funds (No. 2081923028).
- The work was supported by Researchers Supporting Project number (RSPD2024R972), King Saud University, Riyadh, Saudi Arabia.

References

[1] F. Riaz, F.Z. Yam, M.A. Qyyum, M.W. Shahzad, M. Farooq, P.S. Lee, M. Lee, Energies 14 (2021) 2819.
[2] T.O. Alshammari, S.F. Ahmad, M. Abou Houran, M.K. Agrawal, B.P. Pulla, T.U.K. Nutakki, A. Albani, H.M. Youshanlouei, Thermal energy simulation of the building with heating tube embedded in the wall in the presence of different PCM materials, J. Energy Storage 73 (2023) 109134, https://doi.org/10.1016/j.est.2023.109134.
[3] K. Guedri, P. Singh, F. Riaz, A. Inayat, N.A. Shah, B.M. Fadhl, B.M. Makhdoum, A. Arsalanloo, Solidification acceleration of phase change material in a horizontal latent heat thermal energy storage system by using spiral fins, Case Stud. Therm. Eng. 48 (2023) 103157, https://doi.org/10.1016/j.csite.2023.103157.
[4] Y. Chen, L. Feng, S. Shaukat Jamal, K. Sharma, I. Mahariq, F. Jarad, A. Arsalanloo, Compound usage of L shaped fin and Nano-particles for the acceleration of the solidification process inside a vertical enclosure (A comparison with ordinary double rectangular fin), Case Stud. Therm. Eng. 28 (2021) 101415, https://doi.org/10.1016/j.csite.2021.101415.
[5] Y. Xie, T.U. Kumar Nutakki, D. Wang, X. Xu, Y. Li, M. Nadeem Khan, A. Deifalla, Y. Elmasry, R. Chen, Multi-objective optimization of a microchannel heat sink with a novel channel arrangement using artificial neural network and genetic algorithm, Case Stud. Therm. Eng. 53 (2024) 103938, https://doi.org/10.1016/j.csite.2023.103938.
[6] S. Liu, H. Bai, Q. Xu, P. Jiang, S. khorasani, A. Mohamed, Investigations on effect of arrangement of fins on melting performance of vertical PCM enclosure (3D simulation using FVM methods), Alex. Eng. J. 61 (2022) 12139–12150, https://doi.org/10.1016/j.aej.2022.05.047.
[7] M.A. Khan, H.M. Ali, T. Rehman, A. Arsalanloo, H. Niyas, Composite pin-fin heat sink for effective hotspot reduction, Heat Transf. n/a (2024), https://doi.org/10.1002/htj.23016.
[8] R. Rezazadeh, S. Jafarmadar, S. Khorasani, S.R.A. Niaki, Experimental investigation on thermal behavior of non-boiling slug and bubbly two phase-flow in helical tube with spiral, Proc. Inst. Mech. Eng. Part C J. Mech. Eng. Sci. 236 (2021) 3434–3446, https://doi.org/10.1177/09544062211042045.
[9] F. Riaz, K.H. Tan, M. Farooq, M. Imran, P.S. Lee, Sustainability 12 (2020) 8178.

[10] F. Riaz, M.A. Qyyum, A. Bokhari, J.J. Klemeš, M. Usman, M. Asim, M.R. Awan, M. Imran, M. Lee, Energies 14 (2021) 2429.
[11] H. Ge-JiLe, N.A. Shah, Y.M. Mahrous, P. Sharma, C.S.K. Raju, S.M. Upddhya, Radiated magnetic flow in a suspension of ferrous nanoparticles over a cone with brownian motion and thermophoresis, Case Stud. Therm. Eng. 25 (2021) 100915, https://doi.org/10.1016/j.csite.2021.100915.
[12] J. Li, Z.R. Abdulghani, M.N. Alghamdi, K. Sharma, H. Niyas, H. Moria, A. Arsalanloo, Effect of twisted fins on the melting performance of PCM in a latent heat thermal energy storage system in vertical and horizontal orientations: energy and exergy analysis, Appl. Therm. Eng. 219 (2023) 119489, https://doi.org/10.1016/j.applthermaleng.2022.119489.
[13] H. Ayed, A. Arsalanloo, S. Khorasani, M.M. Youshanlouei, S. Jafarmadar, M. Abbasalizadeh, F. Jarad, I. Mahariq, Experimental investigation on the thermo-hydraulic performance of air–water two-phase flow inside a horizontal circumferentially corrugated tube, Alex. Eng. J. 61 (2022) 6769–6783, https://doi.org/10.1016/j.aej.2021.12.024.
[14] K.H. Almitani, N.H. Abu-Hamdeh, A. Golmohammadzadeh, M. Javaheran Yazd, The effect of various forms of the tube cross on the energetic and exergetic analysis of helical tube in tube heat exchangers of an AHU with energy recovery unit in heating mode: injection of vapor/water particles, J. Therm. Anal. Calorim. 144 (2021) 2709–2720, https://doi.org/10.1007/s10973-020-10546-9.
[15] Y. Cao, H. Ayed, H.S. Dizaji, M. Hashemian, M. Wae-hayee, Entropic analysis of a double helical tube heat exchanger including circular depressions on both inner and outer tube, Case Stud. Therm. Eng. 26 (2021) 101053, https://doi.org/10.1016/j.csite.2021.101053.
[16] H. Chater, M. Asbik, A. Mouaky, A. Koukouch, V. Belandria, B. Sarh, Experimental and CFD investigation of a helical coil heat exchanger coupled with a parabolic trough solar collector for heating a batch reactor: an exergy approach, Renew. Energy 202 (2023) 1507–1519, https://doi.org/10.1016/j.renene.2022.11.108.
[17] W. Li, A. Zehforoosh, B. Singh Chauhan, T. Uday Kumar Nutakki, S. Fayaz Ahmad, T. Muhammad, A. Farouk Deifalla, T. Lei, Entropy generation analysis on heat transfer characteristics of Twisted corrugated spiral heat exchanger utilized in solar pond, Case Stud. Therm. Eng. 52 (2023) 103650, https://doi.org/10.1016/j.csite.2023.103650.
[18] A.H. Eisapour, A. Naghizadeh, M. Eisapour, P. Talebizadehsardari, Optimal design of a metal hydride hydrogen storage bed using a helical coil heat exchanger along with a central return tube during the absorption process, Int. J. Hydrogen Energy 46 (2021) 14478–14493, https://doi.org/10.1016/j.ijhydene.2021.01.170.
[19] T. Halawa, A.S. Tanious, On the use of twisting technique to enhance the performance of helically coiled heat exchangers, Int. J. Therm. Sci. 183 (2023) 107899, https://doi.org/10.1016/j.ijthermalsci.2022.107899.
[20] M.J. Hasan, S.F. Ahmed, A.A. Bhuiyan, Geometrical and coil revolution effects on the performance enhancement of a helical heat exchanger using nanofluids, Case Stud. Therm. Eng. 35 (2022) 102106, https://doi.org/10.1016/j.csite.2022.102106.
[21] N. Lebbihiat, A. Atia, M. Arıcı, N. Meneceur, A. Hadjadj, Y. Chetioui, Thermal performance analysis of helical ground-air heat exchanger under hot climate: in situ measurement and numerical simulation, Energy 254 (2022) 124429, https://doi.org/10.1016/j.energy.2022.124429.
[22] S. Missaoui, Z. Driss, R. Ben Slama, B. Chaouachi, Effects of pipe turns on vertical helically coiled tube heat exchangers for water heating in a household refrigerator, Int. J. Air-Conditioning Refrig. 30 (2022) 6, https://doi.org/10.1007/s44189-022-00005-5.
[23] Y. Cao, H. Ayed, A.E. Anqi, O. Tutunchian, H.S. Dizaji, S. Pourhedayat, Helical tube-in-tube heat exchanger with corrugated inner tube and corrugated outer tube; experimental and numerical study, Int. J. Therm. Sci. 170 (2021) 107139, https://doi.org/10.1016/j.ijthermalsci.2021.107139.
[24] J. Yanlin, Y. Han, F. Meng, Y. Wu, L.I. Jiani, Optimization of enhanced heat transfer and flow resistance reduction in twisted petaloid helically coiled tube based on ZS-RSM and NSGA-II, Int. J. Therm. Sci. 197 (2024) 108843, https://doi.org/10.1016/j.ijthermalsci.2023.108843.
[25] H. Chen, H. Moria, S.Y. Ahmed, K.S. Nisar, A.M. Mohamed, B. Heidarshenas, A. Arsalanloo, M. Mehdizadeh Youshanlouei, Thermal/exergy and economic efficiency analysis of circumferentially corrugated helical tube with constant wall temperature, Case Stud. Therm. Eng. 23 (2021) 100803, https://doi.org/10.1016/j.csite.2020.100803.
[26] C. Xie, I.B. Mansir, I. Mahariq, P. Kumar, A. Arsalanloo, R. Muhammad, F. Jarad, Performance boost of a helical heat absorber by utilization of twisted tape turbulator , an experimental investigation, Case Stud. Therm. Eng. 36 (2022) 102240, https://doi.org/10.1016/j.csite.2022.102240.
[27] C. Luo, K. Song, Thermal performance enhancement of a double-tube heat exchanger with novel twisted annulus formed by counter-twisted oval tubes, Int. J. Therm. Sci. 164 (2021) 106892, https://doi.org/10.1016/j.ijthermalsci.2021.106892.
[28] C. Luo, K. Song, T. Tagawa, Heat transfer enhancement of a double pipe heat exchanger by Co-Twisting oval pipes with unequal twist pitches, Case Stud. Therm. Eng. 28 (2021) 101411, https://doi.org/10.1016/j.csite.2021.101411.
[29] C. Yu, H. Zhang, Y. Wang, M. Zeng, B. Gao, Numerical study on turbulent heat transfer performance of twisted oval tube with different cross sectioned wire coil, Case Stud. Therm. Eng. 22 (2020) 100759, https://doi.org/10.1016/j.csite.2020.100759.
[30] W. Zhu, A. Xu, W. Yang, B. Xiong, C. Xie, Y. Li, L. Xu, Y. Shi, W. Lin, Optimal design of annular thermoelectric generator with twisted tape for performance enhancement, Energy Convers. Manag. 270 (2022) 116258, https://doi.org/10.1016/j.enconman.2022.116258.
[31] M.H. Ali, R.E. Jalal, Experimental investigation of heat transfer enhancement in a double pipe heat exchanger with a twisted inner pipe, Heat Transf. 50 (2021) 8121–8133, https://doi.org/10.1002/htj.22269.
[32] M. Fallah Najafabadi, H. Talebi Rostami, M. Farhadi, Analysis of a twisted double-pipe heat exchanger with lobed cross-section as a novel heat storage unit for solar collectors using phase-change material, Int. Commun. Heat Mass Tran. 128 (2021) 105598, https://doi.org/10.1016/j.icheatmasstransfer.2021.105598.
[33] H.R. Kim, S. Kim, M. Kim, S.H. Park, J.K. Min, M.Y. Ha, Numerical study of fluid flow and convective heat transfer characteristics in a twisted elliptic tube, J. Mech. Sci. Technol. 30 (2016) 719–732, https://doi.org/10.1007/s12206-016-0127-4.
[34] S.W. Chang, P.-S. Wu, W.L. Cai, J.H. Liu, Turbulent flow and heat transfer of helical coils with twisted section, Appl. Therm. Eng. 180 (2020) 115919, https://doi.org/10.1016/j.applthermaleng.2020.115919.
[35] C.-C. Wu, C.-K. Chen, Y.-T. Yang, K.-H. Huang, Numerical simulation of turbulent flow forced convection in a twisted elliptical tube, Int. J. Therm. Sci. 132 (2018) 199–208, https://doi.org/10.1016/j.ijthermalsci.2018.05.028.
[36] S. Eiamsa-ard, N. Maruyama, M. Hirota, S. Skullong, P. Promthaisong, Heat transfer mechanism in ribbed twisted-oval tubes, Int. J. Therm. Sci. 193 (2023) 108532, https://doi.org/10.1016/j.ijthermalsci.2023.108532.
[37] H. Itō, Friction factors for turbulent flow in curved pipes, J. Basic Eng. 81 (1959) 123–132.
[38] P. Mishra, S.N. Gupta, Momentum transfer in curved pipes. 1. Newtonian fluids, Ind. Eng. Chem. Process Des. Dev. 18 (1979) 130–137.
[39] Y. Mori, W. Nakayama, Study of forced convective heat transfer in curved pipes (2nd report, turbulent region), Int. J. Heat Mass Tran. 10 (1967) 37–59.
[40] B.K. Hardik, P.K. Baburajan, S. V Prabhu, Local heat transfer coefficient in helical coils with single phase flow, Int. J. Heat Mass Tran. 89 (2015) 522–538, https://doi.org/10.1016/j.ijheatmasstransfer.2015.05.069.
[41] E. Schmidt, Wärmeübergang und Druckverlust in Rohrschlangen, Chem. Ing. Tech. 39 (1967) 781–789.